AJNR

Morphology and dimensions of the thoracic cord by computer-assisted metrizamide myelography.

F Gellad, K C Rao, P M Joseph and R D Vigorito

This information is current as of May 28, 2024.

Morphology and Dimensions of the Thoracic Cord by Computer-Assisted Metrizamide Myelography

Fouad Gellad,[1] Krishna C. V. G. Rao,[1] Peter M. Joseph,[1] and Robert D. Vigorito[2]

Computed tomographic (CT) measurements of the thoracic spine and its contents were obtained in 33 patients undergoing metrizamide myelography for various spinal disorders. Twenty-eight of these patients had symptoms referable to the cervical or lumbar region and form the basis of this study. Five patients had symptoms referable to the thoracic spine. Sagittal and coronal CT measurements of the thoracic cord and subarachnoid space were obtained in all cases. In addition, macroscopic measurements of the thoracic cord were obtained from 10 autopsies for correlation with the CT findings. The technical aspects of the measurements are discussed; the normal morphology of the thoracic cord and thecal sac is presented; and the metrizamide CT pattern associated with pathologic lesions involving the thoracic cord is analyzed.

Computed tomography (CT) is used extensively in the evaluation of spinal disease. Many reports have emphasized the value of CT in lumbar disk disease [1, 2], lumbar stenosis [3, 4], spinal trauma [5, 6], spinal neoplasms [7], and congenital anomalies of the spine [8–10]. Fewer reports have described the morphology of the normal spinal cord [11, 12] and spinal canal [13, 14]. To our knowledge, a detailed CT evaluation of the thoracic cord has not yet been reported.

Materials and Methods

Of 33 patients undergoing metrizamide CT of the thoracic spine, 28 had symptoms related to the cervical or lumbar spine. Normal thoracic cord measurements were obtained from this group. Five patients had symptoms related to the thoracic spine. Twenty patients were male and 13 were female. Ages were 18–79 years (mean, 42 years). Since most of the patients underwent metrizamide myelography before the CT examination, the concentration of metrizamide was 220–300 mg I/ml. CT was performed 1–6 hr after injection of metrizamide. Three patients underwent CT immediately after intrathecal injection of metrizamide (concentration, 170 mg I/ml). All patients were placed in the Trendelenburg position at some point after the injection of contrast medium. All scanning was performed on a GE 8800 CT/T scanner at 120 kVp, 760 mAs. The window width was set at 1,000 Hounsfield units (H) and the window level at 350 H.

An anteroposterior ScoutView film was obtained in each patient for localization of levels for subsequent measurement (fig. 1). The sagittal and coronal measurements of the thoracic cord and subarachnoid space in the axial plane were obtained directly from the CRT at 2× magnification.

In addition, macroscopic measurements of the sagittal and coronal diameters of the thoracic cord were obtained from 10 autopsied patients who died from illnesses other than spinal disease.

Results

The mean sagittal and coronal diameters of the normal thoracic cord are given in table 1 and figure 2. The mean CT diameters of the normal subarachnoid space are given in table 1 and figure 3. The postmortem cord diameters are given in table 2 and figure 4.

The normal spinal cord is round in the thoracic region (fig. 5B), elliptical in the cervical region (fig. 5A), and square in the conus (fig. 6) because of the emerging lumbar nerve roots. The thoracic cord is more ventrally located and the subarachnoid space is wider dorsally than ventrally (fig. 5B). The epidural space is very narrow in the thoracic region (fig.6). The dural sac, a smoothly marginated structure, occupies most of the spinal canal. Differentiation of the gray and white matter of the cord and of the normal spinal canal was not possible on the CT images.

Discussion

CT has markedly improved our understanding of and our diagnostic capabilities in spinal disease. In the thoracic region, plain CT is excellent for evaluating bony lesions due to neoplasm or trauma. However, the contents of the spinal canal are not distinctly identified. The dural sac cannot be differentiated from the epidural space unless there is abundant epidural fat. With current equipment, the cord cannot be differentiated from the subarachnoid space and dura except in the upper cervical region. Evaluation of the thoracic cord requires intrathecal injection of a contrast medium (metrizamide in all our cases). The concentration of the contrast medium is not a critical factor. The thoracic cord can be adequately visualized by CT at concentrations of 170–300 mg I/ml of metrizamide. The time interval between contrast administration and CT scanning is not critical as long as the delay does not exceed 6 hr. Finally, the position of the patient is not critical. Supine and prone positions reveal the same configuration and location of the thoracic cord.

It is generally acknowledged [15, 16] that the choice of window level (WL) can have a significant effect on the measured diameters
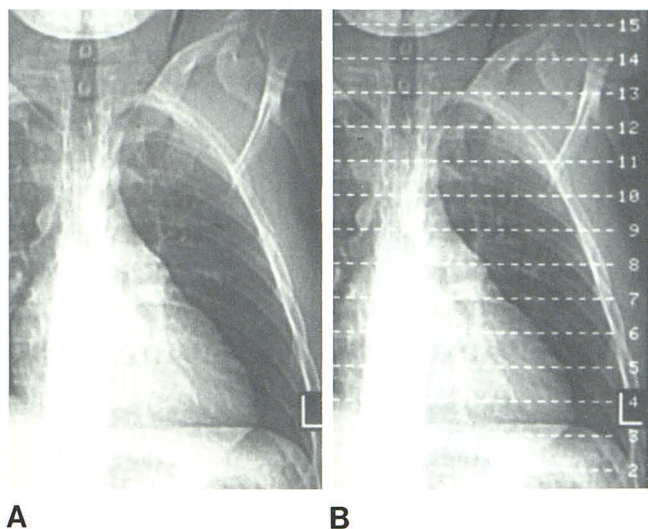

A   **B**

Fig. 1.—Anteroposterior ScoutView images without (**A**) and with (**B**) locations of CT slices obtainable.

TABLE 1: **CT Diameters (Mean ± 2 SD) of Normal Thoracic Cord and Subarachnoid Space in Vivo (n = 28)**

Spinal Level	Diameter of Thoracic Cord (mm)		Diameter of Subarachnoid Space (mm)	
	Sagittal	Coronal	Sagittal	Coronal
T1	6.4 ± 2	9.4 ± 1.6	13.3 ± 2.5	16.4 ± 1.8
T2	5.9 ± 2	8.7 ± 2.5	13.0 ± 2.4	14.9 ± 2.5
T3	6.2 ± 1.8	8.2 ± 2	14.0 ± 2.8	14.1 ± 2.4
T4	6.0 ± 1	8.5 ± 1.2	14.5 ± 2.2	15.7 ± 2.5
T5	6.0 ± 1.6	8.1 ± 1.8	13.0 ± 3.4	13.9 ± 2.8
T6	6.0 ± 1.7	8.2 ± 1.1	13.3 ± 3.2	14.6 ± 2.2
T7	5.9 ± 1.8	8.0 ± 1.2	13.5 ± 3.0	14.2 ± 3.3
T8	6.0 ± 1.6	7.8 ± 1.5	13.2 ± 2.6	13.9 ± 2.7
T9	6.2 ± 1.4	8.0 ± 1.5	13.7 ± 2.8	14.5 ± 2.6
T10	6.0 ± 1.3	8.0 ± 1.5	13.4 ± 2.8	14.4 ± 2.8
T11	6.5 ± 2	8.4 ± 2	14.0 ± 3.4	14.9 ± 3.1
T12	6.8 ± 1.8	8.3 ± 1.7	14.0 ± 3.5	16.3 ± 3.4
L1	5.5 ± 2	6.2 ± 2.5	15.0 ± 3.6	17.0 ± 3.2

TABLE 2: **CT Diameters (Mean ± 2 SD) of Normal Postmortem Thoracic Cord (n = 10)**

Spinal Level	Sagittal Diameter (mm)	Coronal Diameter (mm)
T2	6.8 ± 2.6	11.1 ± 2
T5	6.8 ± 2.6	11.1 ± 2
T8	7.4 ± 2.8	10.5 ± 3
T12	7.2 ± 2	11.7 ± 3.2

of high-contrast objects (such as, in our case, the apparent diameter of the spinal cord surrounded by metrizamide). This effect is equivalent to the point spread effect [17]. The major difference between our technique and that of Siebert et al. [16] and Koehler et al. [15] lies in the choice of window width (WW). Both groups of researchers recommended using a narrow WW and carefully adjusting the WL to a value corresponding to the mean of the CT attenuation value of the spinal cord and the surrounding metrizamide. This requires that

the CT values of the cord and metrizamide be measured and the mean calculated for each image. In our method, on the contrary, a wide WW is used (typically 1,000 H) and the WL is set so that the densities of both the cord and metrizamide lie within the gray-scale range of the viewer. The advantage of this technique is that moderate variations or errors in the selection of the WL do not seriously affect the measured diameters of the cord. The importance of wide WW in judging edge contours has been demonstrated and emphasized previously [18]. We verified these results by measuring the density of selected images at different window settings (WW and WL). At one particular level the cord measured 90 H, while metrizamide varied from 570 H to 715 H within the subarachnoid space. Thus, the desired WL would fall between 330 H and 400 H, depending on what CT value was used for metrizamide.

A preliminary experiment established the reproducibility of diameters measured with the wide-window (WW = 1,000 H) technique. A total of 12 measurements of the sagittal and frontal cord diameters were taken by two observers. The results fluctuated by no more than ±0.03 mm, which corresponds with the pixel size in this image. Thus, the subjective element in judging the cord-metrizamide border is insignificant and unlikely to skew the accuracy of the results. In a second experiment the WL was deliberately changed from 330 H to 400 H, while the WW remained at 1,000 H. As before, the results showed no change greater than the pixel limit of ±0.03 mm.

Koehler et al. [15] stated that WW has no effect on apparent size as long as the WL is carefully adjusted to the mean of the densities of the two regions. This is consistent with our results. Siebert et al. [16] indicated that measurements are most accurate with the narrowest possible WW permitting sharp definition between the two substances (thus minimizing the subjective element in judging the border). However, a narrow WW prevents perception of the spatial gradient and anatomical configuration of the cord-metrizamide border.

The CT density or H value of the thoracic cord in the presence of metrizamide is not at all a well controlled or constant variable. The rate of diffusion of metrizamide into the cord can be expected to vary, even within a given patient, because of different concentration gradients at different levels of the spine [19]. This depends on both the concentration of the metrizamide used and the time interval between the injection and the CT study. Furthermore, physical factors such as beam hardening in bone and iodine [20] are known to influence the reconstructed CT number, even when the density is constant. For these reasons, we believe that a wide WW, which is not critically dependent on the measured CT value of metrizamide, is preferable.

The mean CT dimensions of the sagittal diameter of the cord (table 1) correlate well with the postmortem measurements (table 2). The mean coronal diameters were slightly larger in the postmortem study, presumably because of differences in measurement techniques combined with minimal cord swelling. Overall, the CT dimensions of the thoracic cord are slightly smaller than those reported previously [21]. This is attributed to the in vivo nature of our study, whereas the prior extensive radiographic analysis was a postmortem study involving cord swelling.

We derived the normal range of the thoracic cord dimensions from our normal population. A minor increase in size due to intramedullary tumor or syringomyelia could not have been readily detected. The same is true for a minor decrease in size due to atrophy from radiation or trauma. CT was not useful in differentiating between gray and white matter of the cord. Focal demyelination is not detectable with the present CT equipment.

CT has a definite role to play, however. It can readily differentiate intramedullary from intradural or extradural lesions. The intramed-
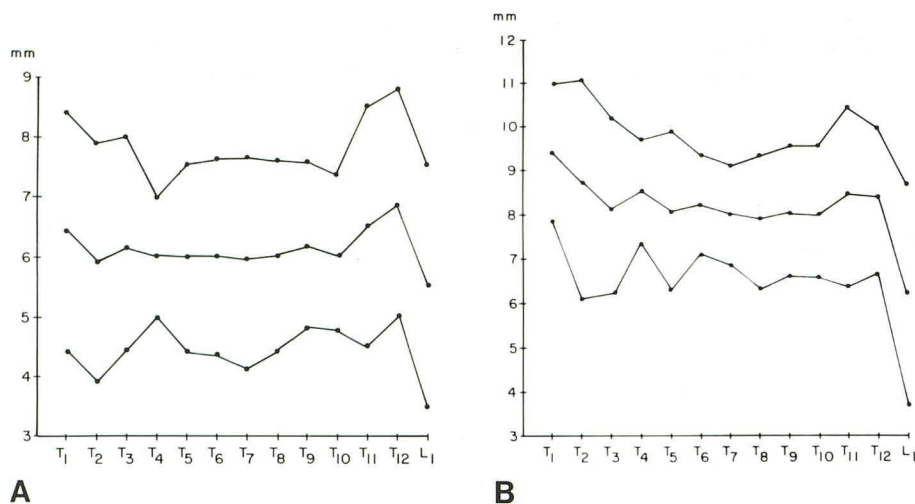
A

B

Fig. 2.—CT sagittal (**A**) and coronal (**B**) diameters of normal thoracic spinal cord in vivo (*n* = 28). Center line = plot of mean values at each level; upper line = mean + 2 SD; lower line = mean − 2 SD.
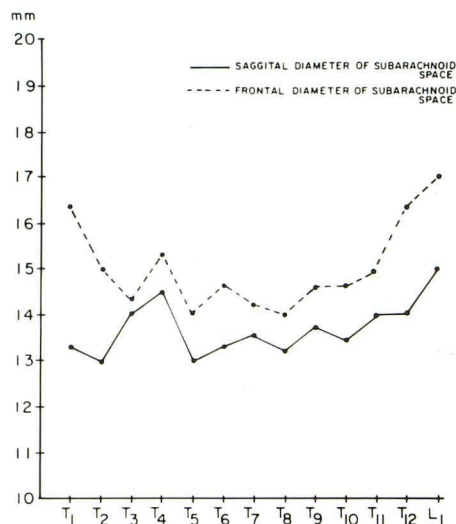

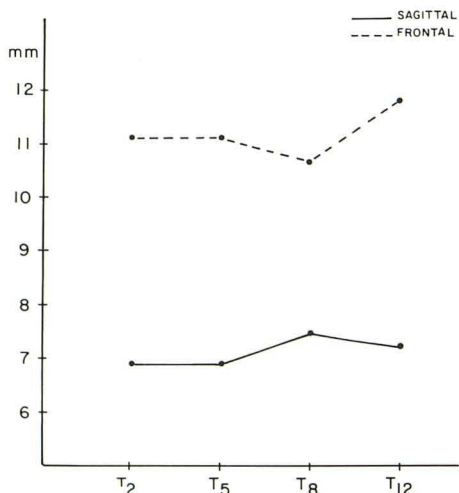Fig. 3.—Mean CT sagittal and frontal diameters of normal subarachnoid space in vivo (*n* = 28).

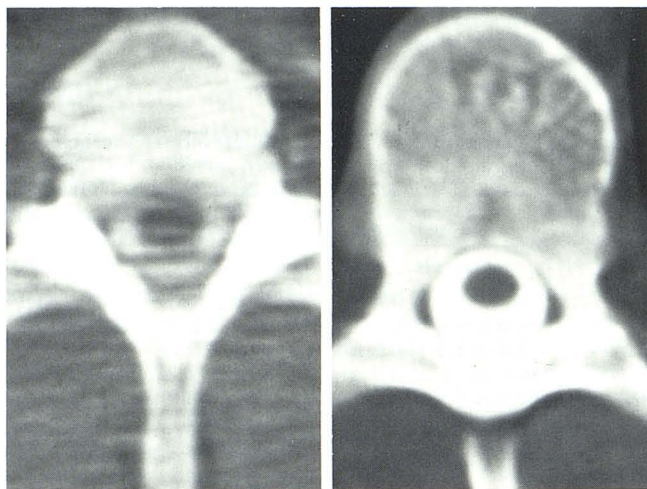A   B

Fig. 5.—CT of normal spinal cord. **A,** Upper thoracic level. Elliptical cord in cross section. "Streak" artifacts from shoulder. **B,** Midthoracic level. Cord is ventrally located within metrizamide-filled subarachnoid space.

Fig. 4.—Mean CT sagittal and frontal diameters of normal postmortem thoracic cord (*n* = 10) at four spinal levels.

ullary lesion produces enlargement of the cord and thinning or even obliteration of the subarachnoid space. The intradural lesion displaces the cord and produces ipsilateral dilatation and contralateral effacement of the subarachnoid space. This lesion can also present as a well defined filling defect in the subarachnoid space, clearly demarcated from the cord outline. Since the dural sac in the thoracic spine is very close to the bony canal, even a small extradural lesion will cause displacement of the thecal sac. In addition, most extradural lesions are associated with bony changes. CT is excellent for demonstrating not only the extradural nature of the lesion but also the paraspinal extension of the disease.

Despite the detailed information provided by CT, myelography remains in many cases the first diagnostic tool for screening and localizing spinal pathologic processes. CT provides an adjunct for more precise evaluation.

Fig. 6.—CT of normal spinal cord at lower thoracic level. Cord is centrally located (A) and appears square in region of conus (B) with narrow epidural space. C, Tip of conus with the emerging dorsal and ventral roots.

A

B

C
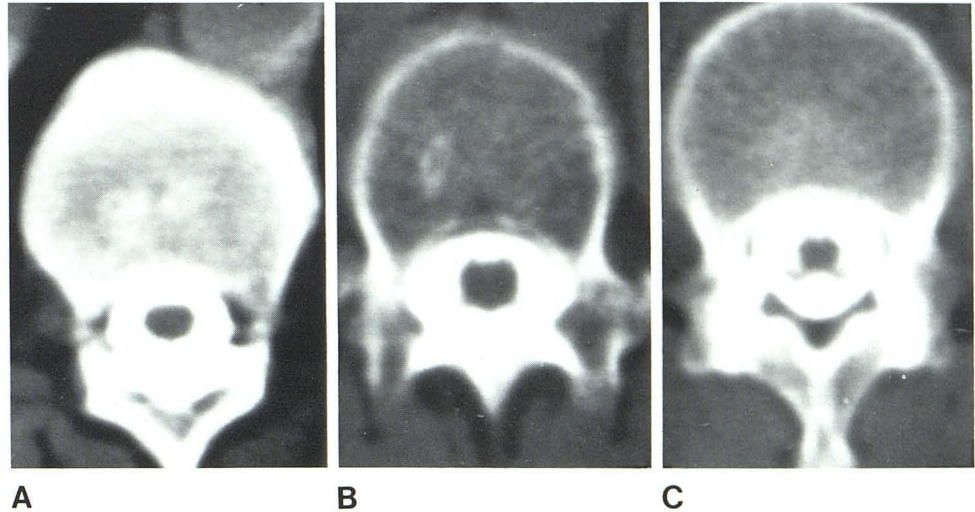
REFERENCES

1. Williams AL, Haughton VM, Syvertsen A. Computed tomography in the diagnosis of herniated nucleus pulposus. *Radiology* **1980**;135:95–99

2. Carrera GF, Williams AL, Haughton VM. Computed tomography in sciatica. *Radiology* **1980**;137:433–437

3. Mikhael MA, Circic I, Tarkington JA, Vick NA. Neuroradiological evaluation of lateral recess syndrome. *Radiology* **1981**;140:97–107

4. Carrera GF, Haughton VM, Syvertsen A, Williams AL. Computed tomography of lumbar facet joints. *Radiology* **1980**;134:145–148

5. Brant-Zawadzki M, Jeffrey RB, Minagi H, Pitts LH. High resolution CT of thoracolumbar fractures. *AJNR* **1982**;3:69–74, *AJR* **1982**;138:699–704

6. Ghoshharja K, Rao KCVG. CT in spinal trauma. *CT* **1980**;4:309–318

7. Resjo IM, Harwood-Nash DC, Fitz CR et al. CT metrizamide myelography for intraspinal and paraspinal neoplasm in infants and children. *AJR* **1979**;132:367–372

8. Resjo IM, Harwood-Nash DC, Fitz CR, Chuang SH. Computed tomographic metrizamide myelography in syringohydromyelia. *Radiology* **1979**;131:405–407

9. Wolpert SM, Scott MR, Carter BL. Computed tomography in spinal dysraphism. *Surg Neurol* **1977**;8:199–206

10. DiChiro G, Doppman JL, Wener L. Computed tomography of spinal cord arteriovenous malformation. *Radiology* **1977**;123:351–354

11. Resjo IM, Harwood-Nash DC, Fitz CR, Chuang S. Normal cord in infants and children examined with computed tomographic metrizamide myelography. *Radiology* **1979**;130:691–696

12. Thijssen HOM, Keyser A, Horstink MWM, Meijer E. Morphology of the cervical spine cord on computed myelography. *Neuroradiology* **1979**;18:57–62

13. Haughton VM, Williams AL. Computed tomography of the spine. St. Louis: Mosby, **1982**

14. Lee BCP, Kazam E, Newman AD. Computed tomography of the spine and spinal cord. *Radiology* **1978**;128:95–102

15. Koehler PR, Anderson RE, Baxter B. The effect of computed tomography viewer controls on anatomical measurement. *Radiology* **1979**;130:189–194

16. Seibert CE, Barnes JE, Dreisbach JN, Swanson WB, Heck RJ. Accurate CT measurement of the spinal cord using metrizamide: physical factors. *AJNR* **1981**;2:75–78

17. Joseph PM. Artifacts in CT scanning. In: Newton TH, Potts G, eds. *Radiology of the skull and brain*. St. Louis: Mosby, **1981**:3956–3992

18. Joseph PM, Stockham CD. The influence of modulation transfer function shape on computed tomographic image quality. *Radiology* **1982**;145:179–185

19. Winkler SS, Sackett JF. Explanation of metrizamide brain penetration: a review. *J Comput Assist Tomogr* **1980**;4:191–193

20. Joseph PM, Spital RD. A method for correcting bone induced artifacts in computed tomography scanners. *J Comput Assist Tomogr* **1978**;2:100–108

21. Nordqvist L. The sagittal diameter of the spinal cord and subarachnoid space in different age groups: a roentgenographic postmortem study. *Acta Radiol [Diagn]* (Stockh) **1964**;227:1–86